Journal of Ovonic Research Vol. 14, No. 4, July – August 2018, p. 277 - 285

INVESTIGATION OF PHOTOVOLTAIC PROPERTIES OF Al_2O_3 SUPPORTED Ni (II)-SCHIFF BASE COMPLEX SYNTHESIZED BY WET CHEMICAL METHOD

D. KILINC[a], O. SAHIN[b], S. HOROZ[c,*]
[a]*Siirt University, Faculty of Arts&Sciences, Department of Chemistry, Siirt, 56100, Turkey*
[b]*Siirt University, Faculty of Engineering and Architecture, Department of Chemical Engineering, Siirt, 56100, Turkey*
[c]*Siirt University, Faculty of Engineering and Architecture, Department of Electrical and Electronics Engineering, Siirt, 56100, Turkey*

In our present study, 5-amino-2, 4-dichlorophenol-3,5-ditertbutylsalisylaldimine ligand, Ni (II)-Schiff Base complex and Al_2O_3 supported Ni (II)-Schiff Base complex were synthesized by wet chemical method. Current density (J)–voltage (V) measurement was performed to investigate the effect of Al_2O_3 support material on the photovoltaic properties of Ni (II) Schiff Base complex. The power conversion efficiencies (η%) for Ni (II)-Schiff Base and Al_2O_3 supported Ni (II)-Schiff Base complexes were calculated as 0,72 and 0.85, respectively. This result suggests that Al_2O_3 supported Ni (II)-Schiff Base complex with ligand which shows higher solar cell performance than pure Ni (II) Schiff based complex, can be used as a sensitizer in DSSC technology. Moreover, the structural, morphological and optical properties of Al_2O_3 supported Ni (II)-Schiff Base complex were characterized by X-ray diffraction (XRD), scanning electron microscope (SEM), Fourier Transform Infrared Spectroscopy (FT-IR) and optical absorption measurements, respectively.

(Received May 26, 2018; Accepted July 26, 2018)

Keywords: Al_2O_3 support material, Characterization, Particle size, Power conversion efficiency, Synthesis

1. Introduction

With the growing energy demand, the depletion of readily available, economical fossil fuel sources create an important intimidation to the global administrations in the future. Due to the devastating environmental effects of classical energy sources, it seems necessary to improve clean energy resources. While thinking the detrimental environmental effects of energy sources, it seems that improving the clean alternative energy sources is a requirement [1-9]. The solar energy, which is the main source of all other energy types, is clean and safe. For this reason, to the most hopeful technique for future low cost power production is transformation of sunlight to electricity utilizing dye-sensitized solar cells (DSSCs) have been worked. DSSC is generally occurred from a semiconductor film mostly TiO_2, mechanic backing covered with a conductive oxide (TCO), a sensitizer, an electrolyte and a counter electrode. [10–13].

Due to their extensive absorption spectra and suitable photovoltaic properties metal complexes have been researched for DSSCs. Absorption of in the visible section of the solar spectrum is caused from a metal to ligand charge transfer (MLCT) stage [14]. Until now, Ru-complexes show the most effective sensitizers [15-18], with different structures. Nevertheless, it was limited heir large-scale applications due to the high cost and rareness of the ruthenium metal. For this reason, it has been replacing Ru based dyes with more economical metal structures such as Ni, Co, Fe, etc. [19, 20].

In this research, we used the new Schiff Base complex which named 5-Amino-2,4-dichlorophenol-3,5-di-*tert*-butylsalisylaldimine Ni complex and its state supported on Al_2O_3 that

*Corresponding author: sabithoroz@siirt.edu.tr

we previously synthesized [21, 22]. This Ni(II)-Schiff Base complex and Al_2O_3 supported Ni(II)-Schiff Base complex were dropped on to titanium dioxide (TiO_2) coated on fluorine doped tin oxide (FTO) conductive glass substrate separately to obtain a sensitizer for the DSCC structure. Current density (J)–voltage (V) measurement was conducted to investigate the photovoltaic properties of TiO_2–Ni(II)-Schiff Base complex as defined in literature [23, 24]. In addition to the photovoltaic properties, the structural, morphological and optical properties of the synthesized complex were characterized by X-ray diffraction (XRD), scanning electron microscope (SEM), Fourier Transform Infrared Spectroscopy (FT-IR) and optical absorption measurements, respectively.

2. Experimental part and characterization

The experiment consists of 3 parts.

The first part: Synthesis of 5-amino-2, 4-dichlorophenol-3,5-ditertbutylsalisylaldimine ligand (See Fig. 1). The steps for synthesizing ligand are as follows; (1) 1mmol of 3,5-ditertbutylsalisylaldimine was dissolved in the 30 ml of ethanol. (2) A few drops of formic acid were added onto mixture. (3) The mixture was refluxed for 6 hours at 80 ^{0}C. (4) The solution was allowed to cool to room temperature. (5) The obtained wet sample was washed a few times with methanol and chloroform then, it was dried in the oven.

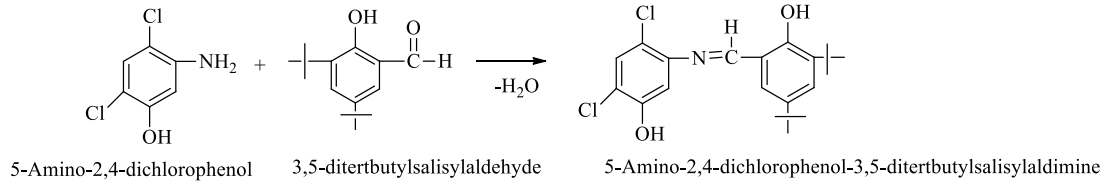

Fig. 1. The structure of the obtained5-amino-2, 4-dichlorophenol-3,5-ditertbutylsalisylaldimine ligand.

The second part: Synthesis of Ni complex with5-amino-2, 4-dichlorophenol-3,5-ditertbutylsalisylaldimine ligand (See Fig. 2). The steps for synthesizing Ni complex with ligand are as follows; (1) The synthesized ligand and nickel (II) chloride hexahydrate were mixed into 20 ml of ethanol solution (Metal (II)-ligand molar ratio was 1:2). (2) Then the same process as above was repeated.

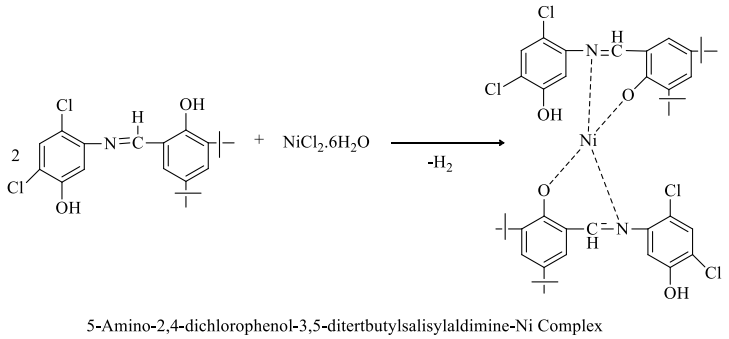

Fig. 2. The structure of Ni complex with5-amino-2, 4-dichlorophenol-3,5-ditertbutylsalisylaldimine ligand.

The third part: Synthesis Al_2O_3 supported Ni (II)-Schiff Base complex (See Fig. 3). The steps for synthesizing Al_2O_3 supported Ni complex are as follows; (1) % 1Ni (II)-Schiff Base complex was slowly added into 0,1 g of Al_2O_3 in ethanol. (2) The new mixture was stirred for 3 hours at room temperature. (4) The solution was filtered and filtrate was heated to a volume of 5

ml. (5) then, it was allowed to cool to room temperature. (6) The obtained wet sample was washed a few times with water then, it was dried in the oven.

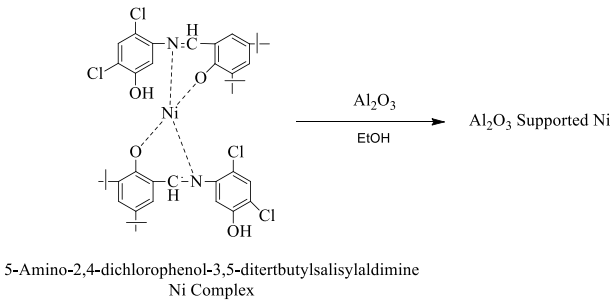

Fig. 3. The structure of Al_2O_3 supported Ni (II)-Schiff Base complex with5-amino-2, 4-dichlorophenol-3,5-ditertbutylsalisylaldimine ligand.

X-ray diffraction (XRD) on a Rigaku X-ray diffractometer with Cu Kα (λ=154,059 pm) radiation and scanning electron microscope (SEM) (JEOL JSM 5800) were used to analyze structural and morphological properties of samples. Electronic absorption spectrums were obtained with a Perkin-Elmer Lambda 2. Current density (J) versus voltage (V) measurement was performed by using PCE-S20 with a monochromatic light source consisting of a 150-W Xe lamp and a monochromator.

3. Results and discussions

XRD analysis

The recorded XRD patterns for Ni (II)-Schiff Base complex with ligand and Al_2O_3 supported Ni (II)-Schiff Base complex with ligand are indicated in the Fig. 4a and Fig. 4b.

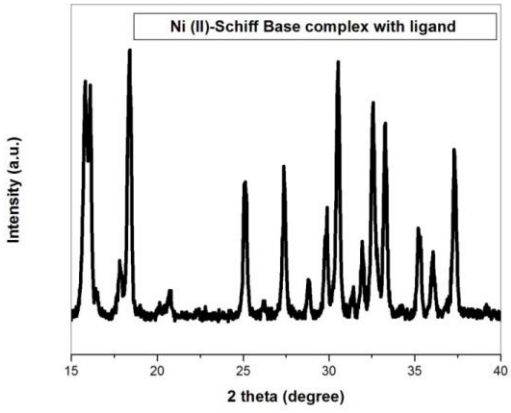

Fig. 4a.The recorded diffraction patterns for Ni (II)-Schiff Base complex with ligand.

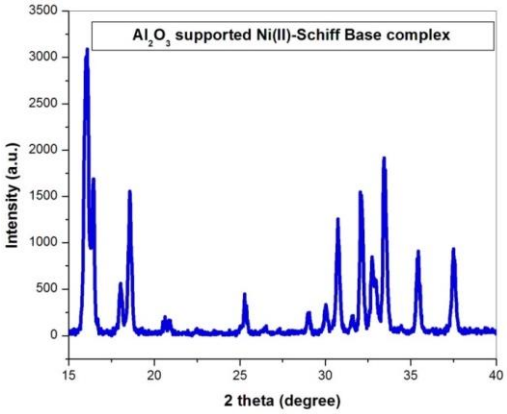

Fig. 4b.The recorded diffraction patterns for Al_2O_3 supported Ni (II)-Schiff Base complex with ligand.

It can be clearly seen that both of samples are in the crystalline phase. Some diffraction patterns for Ni (II)-Schiff Base complex with ligand and Al_2O_3 supported Ni (II)-Schiff Base complex with ligand recorded at 2θ value are given in Table 1.

Table 1. 2θ values corresponding to some diffraction patterns.

2θ values for Ni (II)-Schiff Base complex with ligand (degree)	2θ values for Al_2O_3 supported Ni (II)-Schiff Base complex with ligand (degree)
18.32	18.62
25.11	25.26
30.52	30.74
35.21	35.51

Two important observations should be noted when the given table is considered. The first is the shift in 2θ values corresponding to the diffraction patterns of Al_2O_3 supported Ni (II)-Schiff Base complex. Possible cause of this situation is the result of the interaction between Ni, ligand and Al_2O_3 support. The second is that the particle size of both synthesized samples is slightly different. In other words, Al_2O_3 plays an important role in adjusting the particle size of the Ni complex. Scherre's relation is given in Equation 1 was used to calculate the particle size of Ni (II)-Schiff Base complex and Al_2O_3 supported Ni (II)-Schiff Base complex.

$$d = \frac{k*\lambda}{\beta cos\theta} \quad (1)$$

where; t is calculated grain size of sample, λ is the wavelength of x-ray instrument (0.154 nm), β is the broadening measured as the full width at half maximum (FWHM) in radians, θ is Bragg's diffraction angle and k is constant (its value is usually 0.9). The calculated particle size for Ni (II)-Schiff Base complex and Al_2O_3 supported Ni (II)-Schiff Base complex are approximately 40.03 and 42.23 nm, respectively. This result is an indication that both samples are synthesized in nanoscale.

SEM analysis

Fig. 5a and Fig. 5b demonstrate the recorded SEM images for Ni (II)-Schiff Base complex and Al_2O_3 supported Ni (II)-Schiff Base complex, respectively.

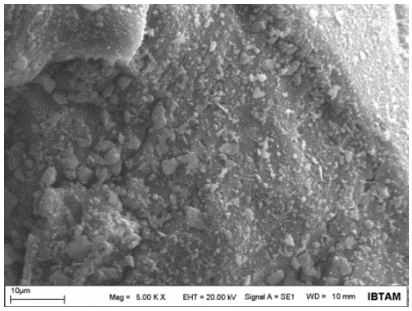

Fig. 5a.The recorded SEM image for Ni (II)-Schiff Base complex.

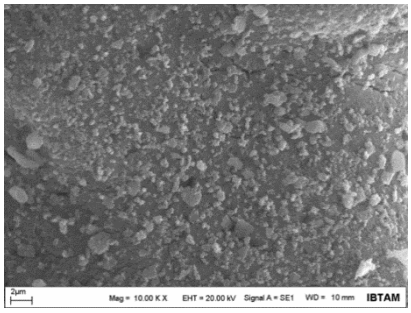

Fig. 5b.The recorded SEM image for Al_2O_3 supported Ni (II)-Schiff Base complex.

A platelet-like structure was observed for both samples. According to Fig. 2b, it can be said that the formation of well-dispersed Al_2O_3 supported Ni (II)-Schiff Base complex can be provided by Al_2O_3 support material. It was also observed that the particle sizes of synthesized samples were less than 100 nm. This result is another indication that both samples are synthesized in nanoscale, is consistent with the calculated particle sizes by Scherrer's relation.

The optical absorption analysis

The optical absorption spectra of 5-amino-2, 4-dichlorophenol-3,5-ditertbutylsalisylaldimine ligand was reported in our previous study [22]. The observed absorption bands at 282 and 377 nm were assigned to n–π∗ transition of the –C=N moiety and π- π^* transition of the phenyl rings, respectively [22, 24]. The recorded optical absorption spectrum for Ni (II)-Schiff Base complex with ligand is indicated in Fig. 6a.

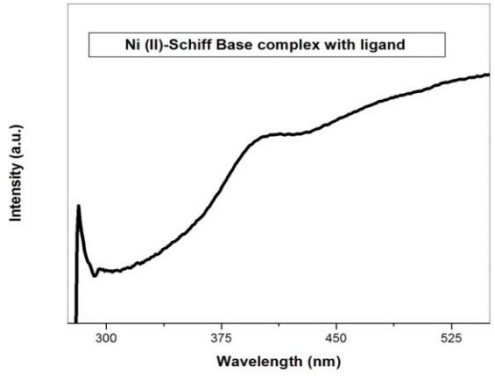

Fig. 6a.The recorded optical spectrum for Ni (II)-Schiff Base complex.

Two optical absorption bands located at 280 and 400 nm were observed. The band at 280 nm can be associated with n–π∗ transition of the azomethine group (–C=N). A shift was observed in the optical absorption spectrum of the complex compared to the ligand. The reason of this shift was explained by Kalita et al. [25]. They reported that nitrogen in the azomethine group is coordinated to Ni ion. Thus, this situation causes a shift in the optical absorption spectrum of Ni (II)-Schiff Base complex with ligand. The band observed at 400 nm can be attributed to d-d or $^3A_{2g}(F)$-$^3T_{1g}$ (F) transition. Similar result was observed by Chouchan [26]. They reported that Ni (II) has an octohedral geometry and Dh symmetry owing to $^3A_{2g}(F)$-$^3T_{1g}$ (F) transition.

Fig. 6b demonstrates optical absorption spectrum for Al_2O_3 supported Ni (II)-Schiff Base complex.

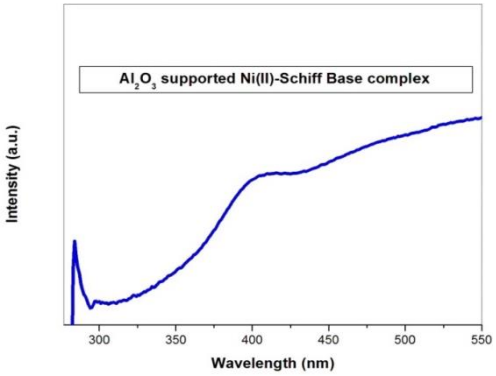

Fig. 6b. The recorded optical spectrum for Al_2O_3 supported Ni (II)-Schiff Base complex.

The recorded Fig. 6a and Fig. 6b are similar. The only difference between the two figures is the shift in the absorption band of Al_2O_3 supported Ni (II)-Schiff Base complex due to Al_2O_3 support material. Two optical absorption bands are located at 283 and 406 nm. These are also associated with n–π∗ and d-d transition, respectively. The reason of the red shift in the absorption band of Al_2O_3 supported Ni (II)-Schiff Base complex could be owing to quantum size effect [27]. Because the particle size of Al_2O_3 supported Ni (II)-Schiff Base complex higher than that of Ni (II)-Schiff Base complex.

J-V analysis

The curves obtained as a result of the J-V measurements carried out to calculate the power conversion efficiencies (η%) for Ni (II)-Schiff Base and Al_2O_3 supported Ni (II)-Schiff Base complexes grown on TiO_2 substrates are shown in Fig. 7. The power conversion efficiency (η) of a solar cell is calculated using the equation given in Equation 2.

$$\eta = \frac{P_m}{P_{in}} = \frac{J_{SC}V_{OC}FF}{P_{in}} \tag{2}$$

where P_m: maximum output power density, P_{in}: power density of incoming light, J_{SC}: short circuit current density, V_{OC}: open circuit voltage, FF: fill factor. The FF can be obtained from the relation is given in the Equation 3.

$$FF = \frac{P_m}{J_{SC}V_{OC}} = \frac{J_{mp}V_{mp}}{J_{SC}V_{OC}} \tag{3}$$

Where J_{mp}: the current corresponding to the maximum power point and V_{mp}: the voltage corresponding to the maximum power point.

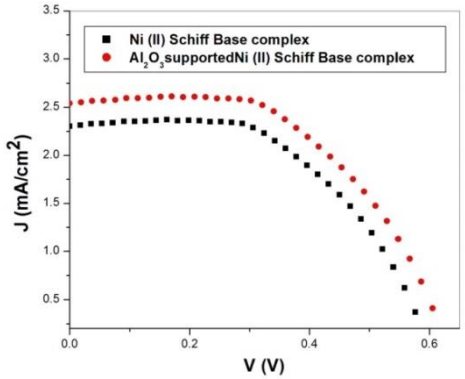

Fig. 7. The recorded J-V curves for Ni (II)-Schiff Base and Al_2O_3 supported Ni (II)-Schiff Base complexes grown on TiO_2 substrates.

η (%) values calculated from the curves shown in Fig. 7 are given in Table 2.

Table 2. Values of V_{OC}, J_{SC} and η% for Ni (II)-Schiff Base and Al_2O_3 supported Ni (II)-Schiff Base complexes grown on TiO_2 substrates.

Samples (complex)	V_{OC} (V)	J_{SC} (mA/cm^2)	η (%)
Ni (II)-Schiff Base	0.57	2.32	0.72
Al_2O_3 supported Ni (II)-Schiff Base	0.60	2.55	0.85

It can be clearly seen thatV_{OC}, J_{SC} and η% values for Al_2O_3 supported Ni (II)-Schiff Base complex are higher than Ni (II)-Schiff Base. The observed higher η% value for Al_2O_3 supported Ni (II)-Schiff Base complex can be assigned with the high number of electrons which are injected into conduction band of TiO_2 from the excited dye of Al_2O_3 supported Ni (II)-Schiff Base complex. Because, it is known well that an increase in number of injected electrons into TiO_2 causes an improvement in the electron injection efficiency and an increase in V_{OC}. Moreover, the Al_2O_3 supported Ni (II)-Schiff Base complex has a wide absoprtion spectral response (see Fig. 6b) which leads to produce more photogenerated excitons in free charge carriers. Hence, this situation results in an increase in J_{SC} value. Thus, it can be said that J_{SC} and V_{OC} values play an important role to improve efficiency of Al_2O_3 supported Ni (II)-Schiff Base complex based DSSC structure. In other words, it is understood that Al_2O_3 supported Ni (II)-Schiff Base complex which shows higher solar cell performance than pure Ni (II) Schiff based complex, can be used as a sensitizer in DSSC technology.

FT-IR analysis

The recorded FT-IR spectra for5-amino-2, 4-dichlorophenol-3,5-ditertbutyl salicylaldimine ligand, Ni (II)-Schiff Base and Al_2O_3 supported Ni (II)-Schiff Base complexes are indicated in Fig. 8.

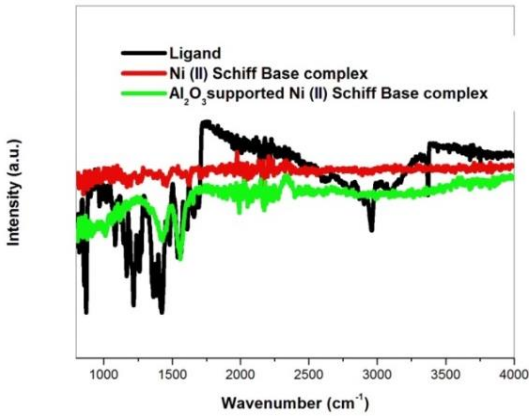

Fig. 8. FT-IR analysis of 5-amino-2, 4-dichlorophenol-3,5-ditertbutyl salicylaldimine ligand, Ni Schiff Base complex and Al_2O_3 supported Ni Schiff base complex.

In Fig. 8 the FT-IR spectrum of 5-amino-2,4-dichlorophenol-3,5-ditertbutyl salicylaldimine ligand, 5-amino-2,4-dichlorophenol-3,5-ditertbutyl salicylaldimine-Ni complex and Al_2O_3 supported 5-amino-2,4-dichlorophenol-3,5-ditertbutyl salicylaldimine-Ni complex were shown at 4000-650 cm^{-1}. The FT-IR spectrum of ligand the peaks seen at 2750-2954 cm^{-1} are because of -CH_3 group. The peak at 1692 cm^{-1} corresponds to the peak of –C=O vibrations. The strong peak at 1607 cm^{-1} corresponds to the peak of the azomethine (C=N) group. In the Ni complex and Al_2O_3 supported nickel complex catalyst frequency of the C=N group were shift at 1621 and 1622 respectively. This shift is because of the nitrogen to the metal. the phenolic C-O in the ligand at 1000-1200 cm^{-1} of display a reduction in their intensity and a shift in the complex slightly that confirm the coordination of the phenolic oxygen to the metal ion. And at 3200 cm^{-1}, caused from -OH group that to be lost in the Ni complex and Al_2O_3 supported nickel complex catalyst.

4. Conclusions

5-amino-2, 4-dichlorophenol-3,5-ditertbutylsalisylaldimine ligand, Ni (II)-Schiff Base complex and Al_2O_3 supported Ni (II)-Schiff Base complex were successfully synthesized by the wet chemical method with previously synthesis procedure [21, 22]. Based on the recorded XRD patterns, the particle sizes of Ni (II)-Schiff Base complex and Al_2O_3 supported Ni (II)-Schiff Base complex were calculated as approximately 40.03 and 42.23 nm, respectively. This result is an indication that the both complexes were synthesized in the nanoscale. An optical absorption band was observed at 400 nm for Al_2O_3 supported Ni (II)-Schiff Base complex. This band could be associated with d-d transition. Morphological studies indicated that the structure of both samples look like a platelet-like structure. J-V measurement was carried out to calculate the η% value for Al_2O_3 supported Ni (II)-Schiff Base complex. The power conversion efficiencies (η%) for Ni (II)-Schiff Base and Al_2O_3 supported Ni (II)-Schiff Base complexes were calculated as 0,72 and 0.85, respectively. This result suggests that Al_2O_3 supported Ni (II)-Schiff Base complex with ligand which shows higher solar cell performance than pure Ni (II) Schiff based complex, can be used as a sensitizer in DSSC technology.

References

[1] R. F. Service, Science **300**, 1219 (2003).
[2] M. Graetzel, Journal of Photochemistry and Photobiology C: Photochemistry Review **4**, 145 (2003).
[3] B. O'Regan, M. Gratzel, Nature **353**, 737 (1991).

[4] G. Redmond, D. Fitzmaurice, M. Graetzel, Chemical Materials **6**, 686 (1994).
[5] M. Chandrasekharam, G. Rajkumar, C. S. Rao, T. Suresh, M. A. Reddy, P. Y. Reddy, Y. Soujanya, B. Takeru, J. H. Yum, M. K. Nazeeruddin, M. Graetzel, Synthetic Metals **161**, 1098 (2011).
[6] M. Chandrasekharam, G. Rajkumar, C. S. Rao, T. Suresh, P. Y. Reddy, Synthetic Metals **161**, 1469 (2011).
[7] W. M. Campbell, A. K. Burrell, D. L. Officer, K. W. Jolley, Coordination Chemistry Reviews **248**, 1363 (2004).
[8] P. Y. Reddy, L. Giribabu, Ch. Lyness, H. J. Snaith, Ch. Vijaykumar, M. Chan- Drasekharam, M. Lakshmikantam, J. H. Yum, K. Kalyanasundaram, M. Graetzel, M. K. Nazeeruddin, Angewandte Chemie International Edition **46**, 373 (2007).
[9] V. Duprez, M. Biancardo, H. Spanggaard, F. C. Krebs, Macromolecules **38**, 10436 (2005).
[10] N. R. Chiou, L. J. Lee, A.J. Epstein, Chemistry of Materials **19**, 3589 (2007).
[11] K. Ocakoglu, S. Okur, Sensors and Actuators B-Chemistry **151**, 223 (2010).
[12] A.D. Becke, Journal of Chemical Physics **98**, 5648 (1993).
[13] C. Lee, W. Yang, R.G. Parr, Physical Review B **37**, 785 (1988).
[14] S. Ardo, G. J. Meyer, Chem. Soc. Rev. **38**, 115 (2009).
[15] C. Y. Chen, M. K. Wang, J. Y. Li, N. Pootrakulchote, L. Alibabaei, C. H. Ngoc-le, J. D. Decoppet, J. H. Tsai, C. Grätzel, C. G. Wu, M. Zakeeruddin, S. M. Grätzel, Nano Lett. **3**, 3103 (2009).
[16] M. Grätzel, J. Photochem. Photobiol. A **3**, 164 (2004).
[17] C. Y. Chen, S. J. Wu, C. G. Wu, J. G. Chen, K. C. Ho, Angew. Chem. Int. Ed. **45**, 5822 (2006).
[18] M. G. Iglesias, J. J. Cid, J. H. Yum, A. Forneli, P. Vázquez, M. K. Nazeeruddin, E. Palomares, M. Grätzel, T. Torres, Energy Environ. Sci. **4**, 189 (2011).
[19] K. Hara, K. Sayama, Y. Ohga, A. Shinpo, S. Suga, H. Arakawa, Chem. Commun. 569 (2001).
[20] L. Schmide-Mende, U. Bach, R. Humphry-Baker, T. Horiuchi, H. Miura, S. Ito, S. Uchida, M. Grätzel, Adv. Mater. **17**, 813 (2005).
[21] D. Kilinc, O. Sahin, C. Saka, Int. J. Hydrogen Energy **42**, 20625 (2017).
[22] D. Kilinc, O. Sahin, C. Saka, Int. J. Hydrogen Energy **43**, 251 (2018).
[23] D. Kilinc, O. Sahin, S. Horoz, Journal of Materials Science: Materials in Electronics, In press (2018) https://doi.org/10.1007/s10854-018-9017-0
[24] D. Kilinc, O. Sahin, S. Horoz, Journal of Ovonic Research **14**, 71 (2018).
[25] M. Kalita, T. Bhattacharjee, P. Gogoi, P. Barman, R. D. Kalita, B. Sarma, S. Karmakar, Polyhedron **60**, 47 (2013).
[26] O. P. Chouchan, G. Jacob, Oriental Journal of Chemistry **30**, 1501 (2014).
[27] G. Schmid, Clusters and Colloids: From Theory to Applications 373 (2007).